Proceedings of the Institute of Acoustics

LOW FREQUENCY VIBRATION INSULATION ON PERIODICALLY STIFFENED PLATES

P Hammer Engineering Acoustics, LTH, Lund University, Lund, Sweden
J Brunskog Engineering Acoustics, LTH, Lund University, Lund, Sweden

1. INTRODUCTION

Among the most difficult problems to handle for light weight floor structures, besides impact sound insulation is vibration isolation against ordinary laundry and dish machines and fan installation. A literature survey in this area results in zero score addressed directly to the problem, however some related studies can be found, e.g. [1-5] penetrating stiffened plates, where [2-3] also considers vibration isolation. Therefor, due to the raised interest of residential housing built-up by light weight floor and wall structures it is judged necessary to penetrate this area. Hence, this paper contains a theoretical study of structural acoustic characteristics of light weight wooden joist floors. A routine to predict the input point mobility is also outlined herein, mainly using the results in [4]. The paper ends with a experimental case study.

Classical vibration isolation theory deals with isolation of a source structure supported on a massless resilient spring. The spring is often assumed blocked at its termination to the receiver structure. This model is often appropriate if the receiver is a heavy concrete plate and if the frequency range of interest pertains to 'massless' springs. But in general the receiver should be included in the analysis, in especially when dealing with lightweight structures as e.g. wooden joist floors.

Taking into account the floor mobility one may end up with an installation design of a one stage isolator, where the mobility mismatch of the aforementioned elements involved is to low. One way to solve this problem is to use two-stage isolators. This may in practise imply an additional rigid mass either directly at the receiver or within the mount itself. The additional mass if appropriate design can then be used as the blocked terminator for the isolator mounted to the source.

This paper is mainly built on the report [7].

2. THE VIBRATION ISOLATION ON AN ARBITRARY PLATES STRUCTURES

The effectiveness of vibration isolation depends on the mobility of the elements involved in a set-up. If the mobility of the receiver structure is low an one-stage isolator can be used with satisfactory results. An example of a application may be a fan mounted on a concrete plate.

The power supplied to a plate structure by a point force is

$$P = \tfrac{1}{2}|F|^2 \operatorname{Re}\{Y_R\}$$

where Y_R is the mobility of the receiver structure and F is the force acting on the receiver structure. Consider Figure 1 a). The power supplied to a plate structure before and after the vibration isolation treatment is

$$P_{before} = \frac{1}{2}\left|\frac{v_0}{Y_R + Y_S}\right|^2 \mathrm{Re}\{Y_R\},\ P_{after} = \frac{1}{2}\left|\frac{v_0}{Y_R + Y_I + Y_S}\right|^2 \mathrm{Re}\{Y_R\}$$

where the isolator mobility Y_I, assumed to be massless, and Y_S is the mobility for the source. The effectiveness, or the insertion loss, of the vibration isolation may be formulated by means of supplied power as

$$E^2 \equiv \frac{P_{before}}{P_{after}}.$$

Thus, a large E indicate a good isolation treatment. In case of one-stage isolation, the effectiveness is

$$E = \left|1 + \frac{Y_I}{Y_R + Y_S}\right| \qquad (1)$$

For the aforementioned concrete plate one often have that $|Y_I| >> |Y_S|, |Y_R|$. Hence, the quotient contributes significantly to E. The more complicated case with light weight floor structures $|Y_R|$ may be in the range of $|Y_I|$ or even higher. Hence, E may be close to one, implying ineffective isolator.

An alternative to "decrease" the receiver mobility may be to use a two-stage isolator. In practise it means that a rigid body, with mobility Y_m, is inserted between two isolators. The formulation of E then becomes

$$E = \left|1 + \frac{(Y_{I1} + Y_{I2})}{(Y_S + Y_R)} + \Delta E\right|,\ \Delta E = \frac{(Y_{I1} + Y_S)(Y_{I2} + Y_R)}{Y_m(Y_S + Y_R)}. \qquad (2)$$

The symbol Y_{I1} and Y_{I2} denotes the isolators connected to the rigid body Y_m, as indicated in *Figure 1 b)*.

Figure 1 a) One-stage isolator, b) Two-stage isolator.

It is clear that a greater included mass, i.e. low Y_m, corresponds to an increase of ΔE and thereby E. Hence, the case of a high receiver mobility may be compensated by means of a rigid mass. In general, however, one desires to obtain the greatest effectiveness given a weight of the rigid mass and total mobility for the isolators. The limit may be set by total static load of the floor and static deflection for the source. From this point of view ΔE may be maximized. If we do so, ΔE_{max} becomes

$$\Delta E_{\max} = \frac{(Y_{I1} + Y_{I2})^2}{4Y_m(Y_S + Y_R)}$$

where the conditions to be fulfilled are $|Y_{I1}| >> |Y_S|$ and $|Y_{I2}| >> |Y_R|$.

Consequently, the aforementioned condition can easily be fulfilled in practise and Y_m may be chosen appropriate. The given consideration in this section demands some knowledge of Y_R. The lack of theoretical data on Y_R has hindered the proper use of the two-stage isolator concept. Hence, in the following section theoretical expressions for the input point mobility of light weight floor is derived, including approximate expressions.

3. INPUT POINT MOBILITY OF A PERIODICALLY STIFFENED PLATE

An infinite, stiffened, thin plate is excited by a point force located in x_0, $F_0\delta(x - x_0)\,\delta(y)\,e^{i\omega t}$.

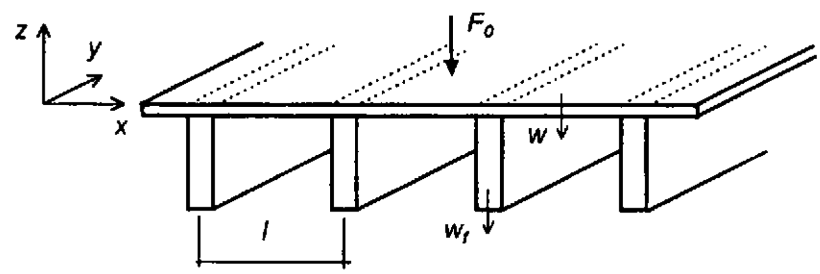

Figure 2 A sketch of the beam reinforced plate.

The time variation $e^{i\omega t}$ will henceforth be suppressed. In the treatments of the governing equations Fourier transform technique will be used. The approach used herein is similar to Mace [1] and Evseev [4]. A similar approach was used by Mace in [5]. The authors has also used the approach [6]. The Fourier transform pair is defined as

$$\tilde{w}(k_x,k_y)=\int_{-\infty}^{\infty}\!\!\int w(x,y)e^{-i(k_x x+k_y y)}dxdy \leftrightarrow w(x,y)=\frac{1}{4\pi^2}\int_{-\infty}^{\infty}\!\!\int \tilde{w}(k_x,k_y)e^{i(k_x x+k_y y)}dk_x dk_y \quad (3)$$

The governing equation for the plate is, in terms of its displacement w_p.

$$B_p\left(\frac{\partial^2}{\partial x^2}+\frac{\partial^2}{\partial y^2}\right)^2 w_p(x,y)-m_p\omega^2 w_p(x,y)=F_0\delta(x-x_0)\delta(y)-p_f(x,y) \quad (4)$$

where B_p in the bending stiffness and mass per unit area of the plate. The pressure $p_f(x,y)$ is the sum of the reaction forces due to the frames. The n:th frame is governed by the Euler-Bernoulli beam equation

$$B_f\frac{d^4 w_{f,n}(y)}{dy^4}-m_f\omega^2 w_{f,n}(y)=F_n(y), \quad (5)$$

where B_f and m_f is the bending stiffness respectively mass per unit length, assumed to be equal for al frames. F_n is the reaction force from the beam acting on the plate. Note that bending moment transmission is neglected. However, as pointed out in [3], this has very little effect of the results in terms of transverse displacement. The boundary conditions at the junction between the plate and the beam are

$$w_{f,n}(y)=w_p(nl,y) \quad (6)$$

This problem was first solve by Evseev [4], by means of Fourier transforming equation (3-6), and taking into account properties of infinite sums and using the Poisson rule. After some manipulations, the transformed displacement can be solved for. With our notations, the transformed displacement can written as

$$\tilde{w}_p(k_x,k_y)=\frac{F_0 e^{i(k_x x_0+k_y y_0)}}{K_p(k_x,k_y)}-\frac{Kf(k_y)F_0}{lK_p(k_x,k_y)}\frac{T_1(k_x,k_y)}{1+\frac{Kf(k_y)}{l}\cdot T_2(k_x,k_y)} \tag{7}$$

where

$$K_p=B_p\left(k_x^2+k_y^2\right)^2-m_p\omega^2,\ K_f=B_f k_y^4-m_f\omega^2 \tag{8}$$

is the spatial stiffnesses of the plate and the frame and

$$T_1(k_x,k_y)=\sum_{m=-\infty}^{\infty}\frac{e^{-i((k_x-\frac{2m\pi}{l})x_0+k_y y)}}{K_p(k_x-2m\pi/l,k_y)},T_2(k_x,k_y)=\sum_{m=-\infty}^{\infty}\frac{1}{K_p(k_x-2m\pi/l,k_y)}$$

Normalising on F_0 and introducing the variables $\alpha = k_x / k_p$, $\beta = k_y / k_p$, $\gamma = k_f / k_p$ leads to, with $Y_0 = 1/8\sqrt{B_p m_p}$, and the abbreviations

$$G_1=(\alpha^4-\gamma^4)\ ,\ G_{2,m}=((\alpha-2m\pi/k_p l)^2+\beta^2)^2-1$$

$$H_1=\frac{B_f k_f^4}{l B_p k_p^4}\sum_{m=-\infty}^{\infty}\frac{e^{-i(\alpha-m2\pi/k_p l)x_0 k_p}}{G_{2,m}},\quad H_2=\frac{B_f k_f^4}{l B_p k_p^4}\sum_{m=-\infty}^{\infty}\frac{1}{G_{2,m}}$$

$$\frac{Y}{Y_0}=\frac{2i}{\pi^2}\int_{-\infty}^{\infty}\!\!\int\left(\frac{1}{\left(\alpha^2+\beta^2\right)^2-1}-\frac{e^{i\alpha x_0 k_p}}{\left(\alpha^2+\beta^2\right)^2}\cdot\frac{H_1\cdot G_1}{1+G_1\cdot H_2}\right)d\alpha\, d\beta\ , \tag{9}$$

where the inverse transform (3 b) has been used, and the receiver is located in the excitation position, $x=x_0$, $y=0$. Equation (9) is an exact expression for the point mobility and for an arbitrarily excitation position. As found out during the progress of this work, the limiting cases for $k_p l$ constitutes valuable results. Hence, for the simplest case, namely if $k_p l \to \infty$, one finds by examine H_1 that $H_1 \to 0$. The remaining term in the integral is the first one. If integrated, one gets the input mobility of an unstiffened plate.

$$Y \to Y_0 \tag{10}$$

If on the other hand we let $k_p l \to 0$, which also implies that $x_0 k_p \to 0$, one gets

$$H_1 \to H_2 \to \frac{B_F k_p^4}{lB_p k_p^4\left(\left(\alpha^2+\beta^2\right)^2-1\right)},\ m=0$$

Inserted in the integral in (9), with $\varepsilon = B_F k_F^4 / \left(lB_p k_p^4\right)$,

$$\frac{Y}{Y_0}\approx\frac{2i}{\pi^2}\int_{-\infty}^{\infty}\!\!\int\frac{d\alpha d\beta}{\left(\alpha^2+\beta^2\right)^2-1+\left(\alpha^4-\gamma^4\right)\varepsilon/\gamma^4}. \tag{11}$$

Introducing the polar co-ordinates $\alpha = \alpha_0 \sin\theta$ and $\beta = \alpha_0 \cos\theta$ and integrating in α_0 by means of residue calculus, equation (12) reduces to

$$Y = Y_0 \frac{1}{2\pi\sqrt{1+\varepsilon}} \int_0^{2\pi} \frac{d\theta}{\sqrt{1+\frac{\varepsilon}{\gamma^4}\sin^4\theta}}. \tag{12}$$

From (12) we get two special cases. If $\varepsilon/\gamma^4 \to 0$, the plate is more bending stiff compared to the frames,

$$Y \approx Y_0 / \sqrt{1+\varepsilon}. \tag{13}$$

If $\varepsilon/\gamma^4 \to \infty$, the frames are more bending stiff compared to the plate. The integral can be rewritten to yield

$$Y \approx Y_0 / \sqrt{1+\varepsilon} \cdot \int^{\pi\left(2\gamma^4/\varepsilon\right)^{1/4}} \frac{d\theta}{\pi} = Y_0 \frac{\gamma\left(2/\varepsilon\right)^{1/4}}{\sqrt{1+\varepsilon}}. \tag{14}$$

Now, by summing up the result we get the following valuable formulae.
<u>$k_p l > 1$</u>: Excitation between frames

$$Y = 1/8\sqrt{m_p B_p}. \tag{15a}$$

Excitation on/near frames

$$Y = (1-i)/\left(4m_F\sqrt{\omega}\left(B_F/m_F\right)^{1/4}\right) \tag{15b}$$

<u>$k_p l < 1$</u>: Arbitrarily excitation point

$$Y = 1/\left(8\sqrt{m_p B_p}\cdot\sqrt{1+B_F k_F^4/\left(lB_p k_p^4\right)}\right); \quad B_F/lB_p \ll 1 \tag{15c}$$

$$Y = \frac{\left(2B_p l/B_F\right)^{1/4}}{8\sqrt{m_p B_p}} \cdot \frac{1}{\sqrt{1+B_F k_F^4/\left(lB_p k_p^4\right)}}; \quad B_F/lB_p \gg 1 \tag{15d}$$

3.1 APPROXIMATE DESIGN OF Y

With the aid of expression (15a-d) one may now introduce an approximative design procedure in order to determine Y. In terms of Helmholtz number for the plate, if $k_p l \leq 0.5$ one may use either expression (15c) or (15d) depending on the quotient ε/γ^4. If $k_p l \geq 1$, expression (15a) or (15b) may be used, depending on the excitation position. If the excitation position is between frames expression (15a) is valid and at or near a frame expression (15b) is appropriate.

For $0.5 < k_p l < 1$ a straight line is draw, connecting the aforementioned expressions. In Figure 3 a) Approximation for Y between frames, *i.e.* excitation point between frames. b) Approximation for Y at/near frames, i.e. excitation point at/near frames and the results are illustrated.

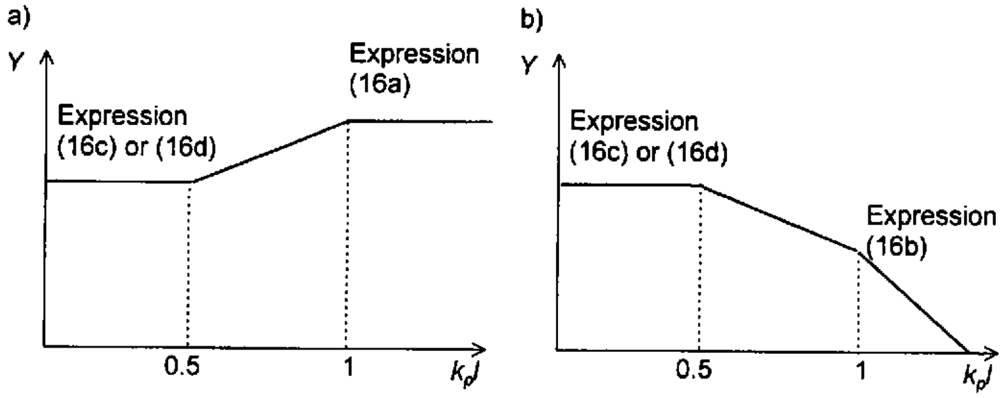

Figure 3 a) Approximation for Y between frames, i.e. excitation point between frames. b) Approximation for Y at/near frames, i.e. excitation point at/near frames

The phase for the case between the frames is zero for all k_pJ. This can of course not be true at low frequency. Separation of peaks due to standing waves both along and between frames causes the phase to vary between $-\pi/2$ and $\pi/2$. This apply for the case in Figure 3 b) as well. But still the magnitude of Y can be quantified satisfactory.

Finally, if we focus on wooden joist floor one can examine the parameters ε/γ^4.

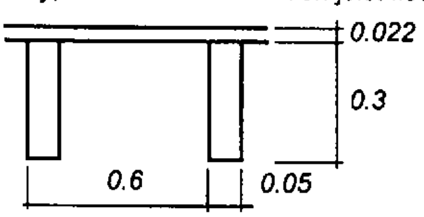

	Chipboard	Wooden joist
E (N/m)	$5\cdot10^9$	$1\cdot10^9$
ρ (kg/m³)	700	610

Figure 4 Example of a wooden joist floor

Using the data given above ε/γ^4 can be calculated. The result is $\varepsilon/\gamma^4 \approx 42 >> 1$. This result is quite representative for wooden joist floors. Consequently, expression (16d) is valid for most wooden joist floors. Experimental verifications of the expressions can be found in [7].

4. A CASE STUDY

This section pertains to a case study of an axial fan mounted on a light weight floor structure. Due to the high mobility of the floor an alternative method to increase the vibration isolation is by means of blocking masses. There are two different principles that one could bear in mind when pertaining to blocking masses. In [1] it is demonstrated that the if the blocking masses is mounted firmly to the receiver structure (floor) it should be concentrated to "points" rather than evenly spread out, to obtain efficient vibration isolation. On the other hand if a soft layer is placed between the blocking mass and the receiver structure, the mass should be spread over a large area as possible. The conclusions are valid provided that the total weight of the blocking mass and stiffness of the layer are constant and if the source mobility is lower than that of the blocking mass. In the case herein presented the later principle has been used where soft springs are imposed between the fan and blocking mass.

4.1 THE FLOOR STRUCTURE AND EXPERIMENTAL SET-UP

As shown in section two the variation of input mobility for the different floor structures considered is in the range 10^{-4} to 10^{-3} m/Ns. A sketch of the pertinent floor is given in figure 4.1. It's impact sound transmission index is 51 dB.

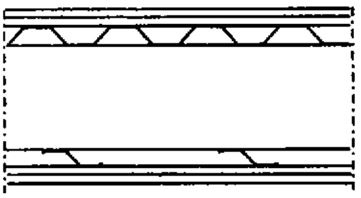

Figure 5 Floor structure under test. The floor is simply supported.

The fan was an axial one with diameter 500 mm and total weight 93 kg. The engine weight was 43 kg. The rotation per minute was 2860 or 48 Hz. Engine power was 7.5 kW.

The floor was mounted between a sending room and receiver room. The volume was 70 respectively 90 m ^{3}. Five different fan mountings was tested, and two are chosen to be presented in the present paper. In the first experiment the fan was freely hinged and had no mechanical contact with the floor structure. Thereby, a situation was created where only air born sound was transmitted. The resultant sound pressure in the receiver room for this case was the compared with that found from the other set-ups. The two set-up to be presented are illustrated below.

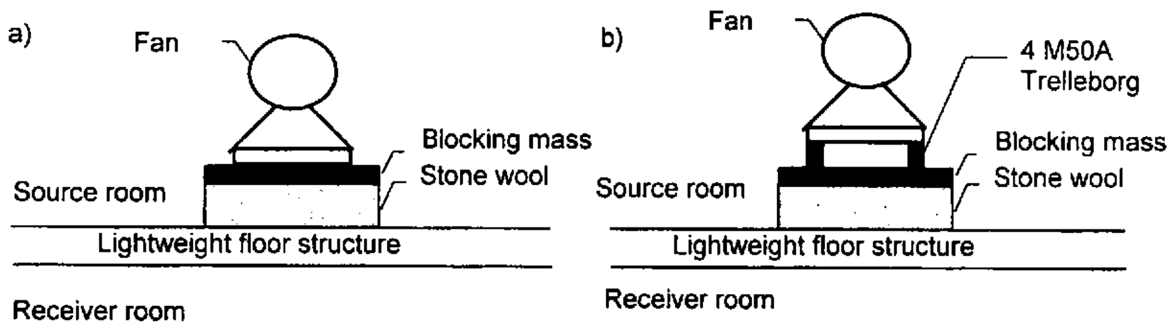

Figure 6 a) Case A. b) Case B.

Data for case A; Blocking masses: Concrete plates 300x300x75 mm. Density 2400 kg/m ^{3}. Total area is 1200x600 mm. Stone wool: 1200x600x120 mm with density 36 kg/m ^{3}.

Data for case B; Blocking masses: Concrete plates 300x300x75 mm. Density 2400 kg/m ^{3}. Total area is 1200x600 mm. Stone wool: 1200x600x120 mm with density 36 kg/m ^{3}.

In the analysis of transmitted sound pressure only translatory motions perpendicular to the floor are considered. The floor input mobility in figure 4.3 is approximated with a constant Y_{floor} = 10 $^{-3}$ m/Ns. The isolators and stone wool are at low frequency considered to act as a pure spring. The blocked resonant frequency between the blocking mass and stone wool is approximately 3 Hz. That for the isolators and fan is approximately 15 Hz.

4.2 RESULTS

The sound pressure level for the different cases are shown in figure 4.7. The peak at 48 Hz in case 2, 3 and 4 is due to the fan engine. The bottom curve , case 1, is the lower limit of the sound pressure level. In the range from 30 - 250 Hz the structure borne sound transmission dominates the sound pressure level. One may even note that for the case with directly mounted fan on floor, a higher sound pressure level at 48 Hz in the receiver room compared with that in the sending room.

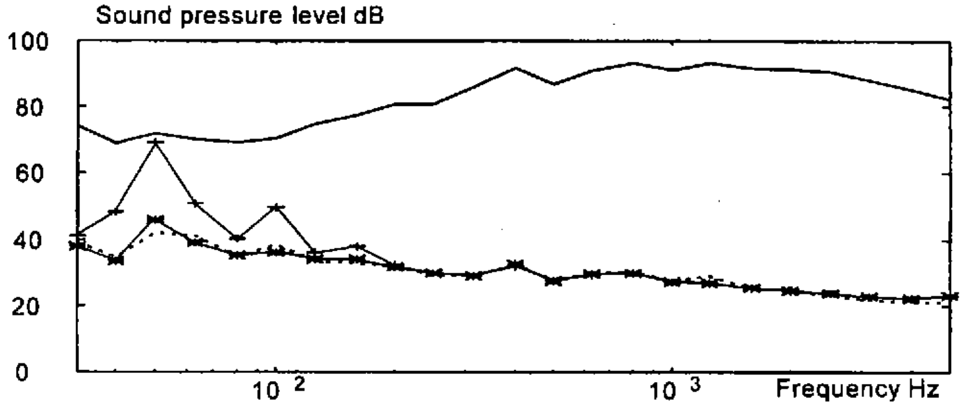

Figure 7 Sound pressure level in receiver room, (+ +) Case A, (* *) Case B, (- - -) only airborne transmission. Sound pressure in the source room (—).*

5. CONCLUDING REMARKS

A simplified design guide for the prediction of point mobility for some typical wooden joist floor is presented. The theoretical and experimental findings agrees well. It is also demonstrated the gain one may expect from using two-stage isolator compared to one-stage isolators. The two-stage isolator, seen from the source, decreases the receiver mobility if the isolator is proper designed. For the experiments case study, the difference between the two aforementioned set-ups is as high as 20 dB at the machine rpm.

6. REFERENCES

1 MACE, B. R. 'Sound radiate from a plate reinforced by two sets of parallel stiffeners' *J. Sound Vib.* **71** (3), pp 435-441, 1980.

2 GOYDER, H.G.D and WHITE, R.G 1980. 'Vibrational power flow from machines into built-up structures. Part I: Introduction and approximate analyses of beam and plate-like foundations.', *J. Sound Vib.*, **68**, pp. 59- 75.

3 CREMER, L., HECKL, M. and UNGAR, E. 1988. Structure - borne Sound. Springer Verlag, Berlin.

4 EVSEEV, V. N. "Sound radiation from an infinite plate with periodic inhomogeneities", *Soviet Physics-Acoustics* **19**, pp 345-351, 1973.

5 MACE, B.R. 1980. 'Periodically stiffened fluid loaded plates I: Response to convected harmonic pressure and free wave propagation. II: Response to line and point forces.', stiffeners' *J. Sound Vib.*, **73**, pp. 473-486.

6 Brunskog, J AND Hammer, P. 'Prediction of impact sound transmission of lightweight floors', Engineering Acoustics, LTH, Lund University, TVBA-3105, Sweden, 1999.

7 HAMMER P. Report "Vibration isolation on light weight floor structures', Engineering Acoustics, Lund University, TVBA-3078, 1996.